

Case study of $\text{Rb}^+(\text{aq})$, quasi-chemical theory of ion hydration, and the *no split occupancies* rule

D. Sabo,^{a,b} D. Jiao,^c S. Varma,^{a,d} L. R. Pratt,^e and S. B. Rempe^{a,*}

Received Xth XXXXXXXXXXXX 20XX, Accepted Xth XXXXXXXXXXXX 20XX

First published on the web Xth XXXXXXXXXXXX 200X

DOI: 10.1039/b000000x

Quasi-chemical theory applied to ion hydration combines statistical mechanical theory, electronic structure calculations, and molecular simulation, disciplines which are individually subjects for specialized professional attention. Because it combines activities which are themselves non-trivial, quasi-chemical theory is typically viewed with surprise. Nevertheless, it provides a fully-considered framework for analysis of ion hydration. Furthermore, the initial calculations are indeed simple, successful, and provide new information to long-standing experimental activities such as neutron diffraction by hydrated ions. Here we review quasi-chemical theory in the context of a challenging application, $\text{Rb}^+(\text{aq})$.

1 Introduction

Water is a chemically active liquid. Probably the most primitive aspect of that chemical activity is dissolution of electrolytes, and the chemical processes based on availability of dissolved ions. One example is salt as a trigger of autoimmune disease.¹⁻⁴ Another example, presumably related to the first,^{5,6} is the selective transport of dissolved ions across membranes.⁷⁻⁹ Rubidium (Rb^+) is interesting in this respect because it serves as an analog of potassium (K^+) that conducts current through potassium ion channels, even though Rb^+ is slightly larger (by 0.2 Å).^{10,11}

In addition to this chemical activity, water has long been a serious challenge for statistical mechanical theory of liquids, which itself is properly almost entirely classical mechanical theory.¹² The challenge presented by liquid water is the variety of intermolecular interactions that must be considered with a wide range of interaction strengths (Fig. 1).¹³ Those interactions include excluded-volume repulsions, essential since liquids and liquid water are dense materials. Those interactions also include H-bonding interactions that are attractive on balance, much stronger than thermal energies, and essential for the characteristic behavior of liquid water.

Attractive interactions that involve *many* neighbors are

^a Center for Biological and Material Sciences, Sandia National Laboratories, Albuquerque, NM 87123, USA

^b Department of Chemistry, New York University, New York, NY USA; E-mail: dubravko.sabo@nyu.edu

^c Texas Advanced Computing Center, University of Texas, Houston, TX USA; E-mail: jjiao@tacc.utexas.edu

^d Department of Cell Biology, Microbiology and Molecular Biology, University of South Florida, Tampa, FL USA; E-mail: svarma@usf.edu

^e Department of Chemical & Biomolecular Engineering, Tulane University, New Orleans LA 70118, USA; E-mail: lpratt@tulane.edu

* Correspondence may be sent to: slrempe@sandia.gov

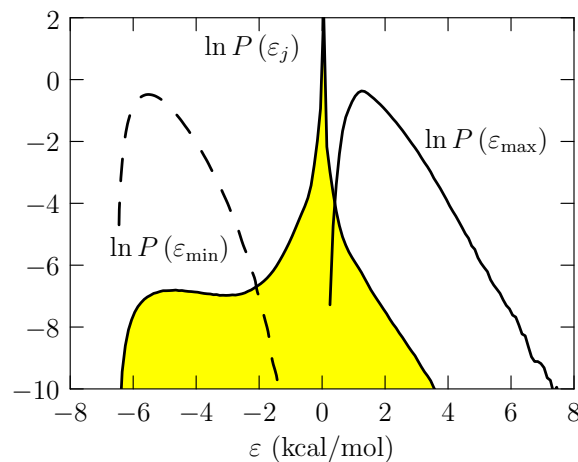


Fig. 1 Probability densities for pair contributions to the binding energy of a water molecule to liquid water.¹⁴ Rightmost curve: the most positive (unfavorable) pair contribution; leftmost curve: the most negative (favorable) contribution. The middle curve (with yellow-shaded area) is the probability density of all the pair interaction contributions.¹⁵

good candidates for treatment by mean-field approximations.^{16,17} Of course, if those attractive interactions are individually weak on a thermal energy scale, that characteristic is favorable for simple theories also.

Here we consider rubidium dissolved in aqueous solution, $\text{Rb}^+(\text{aq})$, to provide a contrast with theories of liquids more broadly,^{16,17} and to pursue a specific discussion of what is yet required theoretically to treat solvated electrolytes. The hydration free energy of $\text{Rb}^+(\text{aq})$ is known to be roughly $-100k_B T$ under standard conditions, favorable enough to dissolve sim-

ple Rb^+ salts, and indeed large on the thermal energy scale. Additionally (Fig. 2), the number of near-neighbors is modest, between four and seven. As another contrast, the isoelectronic $\text{Kr}(\text{aq})$ has about eighteen (18) near-neighbors.^{18,19} From this comparison it is clear that the features of strong attractive interactions and a reduced number of near-neighbors are correlated: the reduced number is a consequence of the crowding of near-neighbors drawn close by the interesting attractive interactions.

This discussion suggests that we seek a way forward by focusing on the *small* number of near-neighbors, deploying direct quantum mechanical computation for $\text{Rb}(\text{H}_2\text{O})_n^+$ with a small number n of neighbors, then stitching those computational results into the broader theory of liquids. That was indeed the idea of quasi-chemical theory discussed here. At a formal level that theory is fully conclusive, but it is surprising that it was not worked-out until fairly recently.^{20–25} It was also surprising that the initial applications of the theory, to $\text{Li}^+(\text{aq})$,²⁶ were highly effective – predictions of hydration free energy matched experiment²⁷ and *ab initio* molecular simulation estimates.²⁸ Further, the initial applications provided new information to long-standing neutron diffraction work on hydrated ions,²⁹ and indeed motivated renewed effort on those experiments.³⁰

The initial applications of quasi-chemical theory could be understood on a physical and intuitive basis. That encouraged the generation of simple mimics that were less fully thought through. A focused discussion of the statistical thermodynamic formalities was given by Asthagiri, *et al.*,³¹ with the intention of reducing the confusion that can result from a crowd of imitators. The presentation of Asthagiri, *et al.*³¹ will be the basis of the discussion that follows.

2 Theory

The primary theoretical target for quasi-chemical theory has been the *excess* (or *interaction part*) of the partial molar Gibbs free energy (or *chemical potential*) of the species of interest, here the $\text{Rb}^+(\text{aq})$. This $\mu_{\text{Rb}^+}^{(\text{ex})}$ is indeed a basic characteristic of the solution and the Rb^+ ion in it, but it is also comparatively simple. The potential distribution theorem¹² offers a partition function for evaluation utilizing information obtained on the local environment of the ion. It is found that the desired free energy can be cast as

$$\mu_{\text{Rb}^+}^{(\text{ex})} = -kT \ln K_n^{(0)} \rho_{\text{H}_2\text{O}}^n + kT \ln p_{\text{Rb}^+}(n) + \mu_{\text{Rb}(\text{H}_2\text{O})_n^+}^{(\text{ex})} - n\mu_{\text{H}_2\text{O}}^{(\text{ex})}. \quad (1)$$

On the right side, notice the reference to the molecular complex $\text{Rb}(\text{H}_2\text{O})_n^+$ and its excess free energy $\mu_{\text{Rb}(\text{H}_2\text{O})_n^+}^{(\text{ex})}$; the

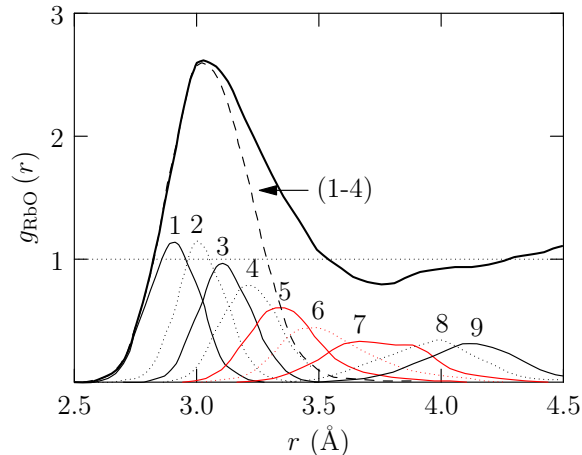
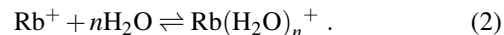


Fig. 2 *Ab initio* molecular dynamics (AIMD) result for the radial distribution of water oxygens about Rb^+ , g_{RbO} . We used VASP-version 4.2,^{32,33} with the Perdew-Wang (PW91) exchange-correlation functional,^{34,35} a plane-wave basis set cutoff at 36.75 Ry with the interaction between valence and core electrons described by the projector augmented-wave method (PAW).³⁶ Corrections to capture long-ranged interactions like dispersion have not been included, and recent studies of ions in water suggest that they are not helpful.³⁷ The system consisted of one Rb^+ ion and 64 waters in a cubic simulation cell with edge length of 12.417 Å and full periodicity. Charge balance was achieved with a neutralizing background. All hydrogen atoms in the system were replaced by deuterium. The simulation was carried out for 49.28 ps with a time step of 0.5 fs. The average temperature during the simulation was 347.9 ± 4.5 K, set intentionally high to avoid the over-structuring of pure water observed in room temperature AIMD simulations.^{38–41} The numbered curves show a neighborhood analysis from decomposing g_{RbO} – curves in red highlight waters that occupy an intermediate region distinct from the first $n=1-4$ waters that fill in the peak of the first maximum, and more distant waters that mostly occupy the second maximum. Results over longer length-scales are shown in Fig. 4.

treatment of the complex itself as a chemical constituent is a characteristic feature of this quasi-chemical theory.^{12,22,24,25}

Other features of Eq. (1) properly fill-in a picture of the chemical equilibrium of this complex. The combination $\mu_{\text{Rb}(\text{H}_2\text{O})_n^+}^{(\text{ex})} - n\mu_{\text{H}_2\text{O}}^{(\text{ex})}$ begins a free energy balance for the association reaction



Similarly,

$$K_n^{(0)} = \frac{\rho_{\text{Rb}(\text{H}_2\text{O})_n^+}}{\rho_{\text{Rb}^+} \rho_{\text{H}_2\text{O}}^n}, \quad (3)$$

with ρ_X the number density of species X, is the equilibrium ratio for that association reaction (Eq. (2)) treated as in an ideal

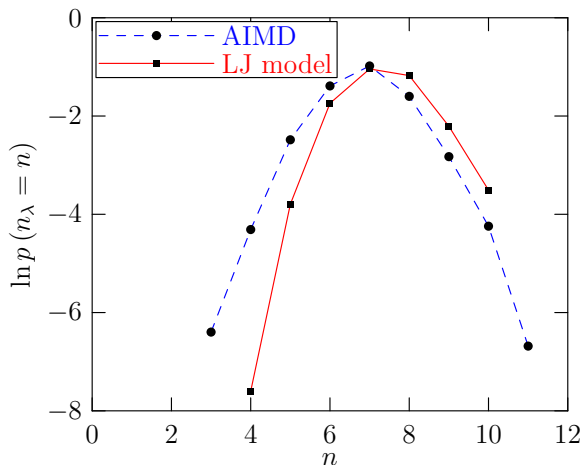


Fig. 3 The coordination number distribution, for the inner-shell radius of $\lambda = 3.76$ Å, from the AIMD simulations and an “LJ model.” For the LJ model, we used Åqvist Lennard-Jones parameters⁴² for the Rb^+ ion, ($\epsilon = 1.71 \times 10^{-4}$ kcal/mol, $\sigma = 5.62177$ Å), and the SPC/E potential⁴³ for water intermolecular interactions. We carried out standard NVT molecular dynamics calculations using the GROMACS⁴⁴ package (version 3.1.4). The system consisted of one Rb^+ and 2177 water molecules in a $(40 \text{ Å})^3$ cell. A single Cl^- was included for charge balance. For electrostatic interactions, the particle mesh Ewald technique was implemented with Fourier spacing of 1.5 Å, a sixth-order interpolation, a 10 Å cutoff in a direct space, and a tolerance of 10^{-5} . A cutoff distance of 16 Å was adopted for the Lennard-Jones interactions. Intramolecular geometric constraints on water molecules were enforced by the SETTLE algorithm.⁴⁵ Data was collected during a 1.0 ns production phase, following a 1.0 ns equilibration phase. The Nose-Hoover thermostat with a coupling constant of 0.2 ps maintained $T = 298.15$ K.^{46–48} The variation in coordination number n is substantially smaller for the LJ model data than for the AIMD results; but remember that the AIMD results correspond to the slightly higher $T \approx 350$ K.

gas, *i.e.*, neglecting interactions with the solution external to the complex; that is signified by the superscript zero. As emphasized previously,^{12,22,31} $K_n^{(0)}$ is a well-defined few-body computational target, and the full force of available quantum mechanical computational methods can be brought to bear. This has been especially relevant to treatment of transition metal ions where d-orbital splitting may be addressed,²⁴ and where the simplest applications of the present theory are particularly effective.^{49,50} Electronic charge-transfer between ion and ligands is another effect of quantum-mechanical origin that is transparently and simply included in these quasi-chemical approaches. Proper accounting of electronic charge density is important for computing absolute and relative ion binding affinities, which is useful for probing mechanisms of selective ion binding.⁵¹

The remaining feature of Eq. (1) is the probability $p_{\text{Rb}^+}(n)$ of observing n ligands within a defined inner shell (Fig. 3). That inner shell is a fundamental concept for this approach, and we return below to discuss it further. For now, note that if only one coordination number n were ever observed, then $p_{\text{Rb}^+}(n) = 1$ and that contribution in Eq. (1) would vanish. Ultimately, that contribution in Eq. (1) carries the full thermodynamic effect of whatever actual variability of inner-shell occupancy does occur.

Leaving the occupancy probability for general consideration, the left side of Eq. (1) is independent of n , and Eq. (1) therefore describes the n -dependence of the probability $p_{\text{Rb}^+}(n)$. If our goal is to evaluate the free energy, however, we can choose n for our convenience. An interesting choice is $n = \bar{n}$, the most probable value (Fig. 4). This choice makes the negative contribution $kT \ln p_{\text{Rb}^+}(n)$ as small as possible, and suggests neglecting that contribution to obtain the convenient approximation

$$\mu_{\text{Rb}^+}^{(\text{ex})} \approx -kT \ln K_{\bar{n}}^{(0)} \rho_{\text{H}_2\text{O}}^{\bar{n}} + \mu_{\text{Rb}(\text{H}_2\text{O})_{\bar{n}}}^{(\text{ex})} - \bar{n} \mu_{\text{H}_2\text{O}}^{(\text{ex})}. \quad (4)$$

The neglected contribution is negative, and the approximate result Eq. (4) will be higher than the true free energy. Nevertheless, a specific evaluation of $p_{\text{Rb}^+}(\bar{n})$ can be straightforwardly extracted from standard molecular simulations,^{52,53} and thus the significance of fluctuations of composition of the inner shell is obtained merely by noting the size of the neglected $kT \ln p_{\text{Rb}^+}(\bar{n})$. Those results are obtained and discussed below.

3 Application to $\text{Rb}^+(\text{aq})$

The primitive quasi-chemical theory, Eq. (4), has indeed been applied to several hydrated metal ions^{26,50,54–57} as well as other solvation problems.^{58–62} For transition metals, as examples, the near-neighbor water molecules are clearly located on the basis of chemical considerations,⁴⁹ and this theory is straightforwardly successful. Generic procedures for those standard cases were given by Pratt and Asthagiri.²⁴ For other cases, some physical judgement is required, and evaluation of the various contributions to Eq. (1) requires analysis. We consider application to $\text{Rb}^+(\text{aq})$ to show how that goes.

3.1 No split occupancies

It is important that theories teach how to understand physical problems in addition to reproducing numerical values of central properties. For our present problems, that learning is focused on how to categorize near-neighbor water molecules to make simple theories effective.

For cases like Rb^+ , in contrast to transition metals, the important observations arise from the AIMD simulation results

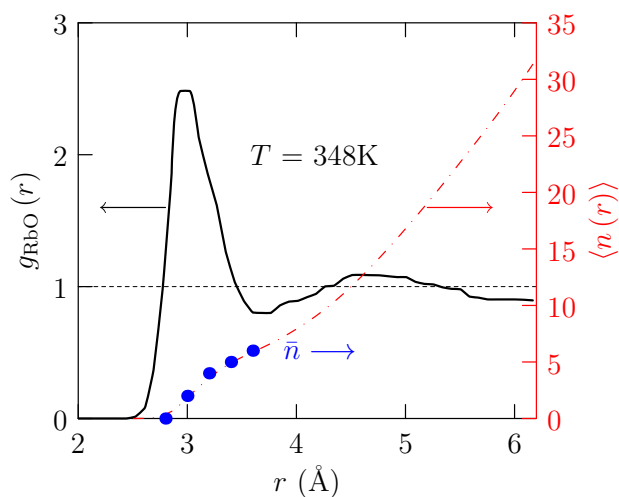


Fig. 4 Distribution $g_{\text{RbO}}(r)$ of oxygen (O) atoms radially from the Rb^+ ion in the AIMD simulation, emphasizing the variation of the most probable occupancy (\bar{n} , the blue dots) of the spherical inner shell defined by the indicated radius r . \bar{n} , being integer-valued, changes discontinuously with defining radius, but reliably tracks the mean number of oxygen atoms within r , *i.e.*, $\langle n(r) \rangle = 4\pi\rho_{\text{O}} \int_0^r g_{\text{RbO}}(x)x^2 dx$ for water at density ρ_{O} . For example, $\langle n(r) \rangle = 6.86 \pm 0.21$ and $\bar{n} = 7$ at $r = 3.76$ Å for AIMD compared to 7.43 ± 0.22 and 7 from the LJ model. Nevertheless, note that $\langle n(r) \rangle$ does not exhibit a convincing plateau for physical identification of a coordination number because the principal minimum of g_{RbO} near $r = 3.76$ Å is weak.

of Fig. 2. The first minimum of the radial distribution is remarkably mild and does *not* provide a convincing identification of an inner shell. Instead, we consider the neighborhood decomposition of that radial distribution. We see that the 7th-most nearest neighbor ($n=7$) contributes to the first maximum (with negligible contribution to the peak), the second maximum, and the first minimum. In other words, the contribution of the 7th-most distant water neighbor to $g(r)$ is multi-modal.

To make our problem simple, we try to set an inner-shell volume so that the 7th neighbor does not contribute. We see from Fig. 5 that $p_{\text{Rb}^+}(n=7)$ is particularly small for an inner-shell radius of $\lambda = 3.2$ Å. With the indicated choice of inner hydration shell, we notice further that neighbors 1-4 fill-out the principal maximum of that radial distribution function.

This lesson we will call the *no split occupancies* rule. These neighborhood analyses⁶³ have become characteristic of quasi-chemical theories and were used previously for $\text{Li}^+(\text{aq})$, $\text{Na}^+(\text{aq})$ and $\text{K}^+(\text{aq})$.^{25,29,56,57,59}

3.2 Methods

To evaluate the quasi-chemical free energy contributions to $\mu_{\text{Rb}^+}^{(\text{ex})}$, we start with the first term of Eq. 4. This term gives the free energies for association of Rb^+ with n water ligands to form clusters within our choice of inner-shell radius ($\lambda = 3.2$ Å). These clustering equilibria take place in an ideal gas with a water density corresponding to a pressure of 1 atm.

Gas-phase thermochemical data required for the association reactions (Eq. (2)) were obtained by electronic structure calculations using the Gaussian09 program⁶⁴ and density functional theory with Becke’s three-parameter exchange functional⁶⁵ and the LYP⁶⁶ electron correlation function (B3LYP). All structures were fully optimized with a basis including polarization and diffuse functions (6-311++G(2d,p)) on oxygen and hydrogen centers, and the LANL2dz effective core potential and basis set on Rb^+ . At the lowest-energy geometry, confirmed by zero-valued slopes of the electronic energy with respect to atomic displacements, a standard Hessian analysis was performed to compute normal mode vibrational frequencies^{67,68} using the same basis set. Quantum mechanical partition functions were then calculated,⁶⁹ thus providing a determination of the free energy changes of the association reactions due to atomic motions internal to water and the clusters at temperature $T = 298$ K and 1 atm pressure.

In a subsequent step, the *cluster results* were adjusted with a *ligand replacement* contribution, $n \ln \rho_{\text{H}_2\text{O}}$, to account for the actual concentration of water ligands in liquid water at the density $\rho_{\text{H}_2\text{O}} = 1$ g/cm³. If this density is tracked as an adjustment of the ideal gas pressure, then it corresponds to a pressure factor of 1354 atm.

To compute the last two terms of Eq. (4), $\mu_{\text{Rb}(\text{H}_2\text{O})_n}^{(\text{ex})} -$

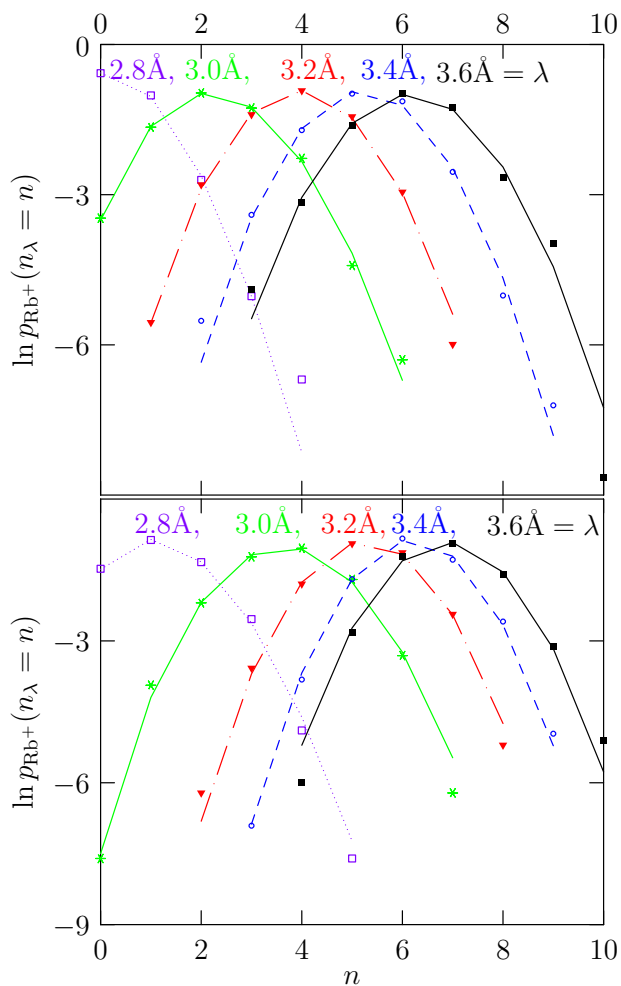


Fig. 5 Coordination number distributions within inner hydration shells defined by various λ : upper AIMD, lower LJ model. The AIMD results display a modest but distinct tendency toward lower coordination numbers. This is possibly connected to the generally incorrect description of overlap repulsions by LJ interactions.

$n\mu_{\text{H}_2\text{O}}^{(\text{ex})}$, we treated the solvent external to individual water ligands and the inner-shell clusters as a reaction field using a polarizable continuum model (PCM).⁷¹ We subtracted the gas-phase electronic structure energy for the n -coordinate cluster geometry to obtain the desired excess free energies. These two terms combined make up the *outer-shell electrostatics* contribution. Finally, we evaluated Rb^+ hydration free energy, $\mu_{\text{Rb}^+}^{(\text{ex})}$, by summing the quasi-chemical components for formation of the most probable complex (Eq. 4), $\text{Rb}(\text{H}_2\text{O})_{\bar{n}}^+$.

The integral equation formalism (IEF-PCM) was implemented for the outer-shell electrostatics calculations.⁷² A radius of 3.2 Å around Rb^+ defined the inner-shell boundary. In addition, default parameters were used to define hydrogen and oxygen radii used to create the solute cavity as a set of overlapping spheres. The dielectric constant of the outer-shell medium was set to 78.35 to represent liquid water.

4 Results

The principal maximum of the Rb-O radial distribution function (Fig. 2) is near $r \approx 3.0$ Å. Experimental studies report similar results for the location of this maximum:^{73–75} 2.93 ± 0.3 Å, 2.90 Å, and 3.05 Å.

The free energy results (Fig. 6) show that the coordination number $n = 4$ is indeed the most probable within the inner hydration shell defined by $\lambda = 3.2$ Å. This then implies $\mu_{\text{Rb}^+}^{(\text{ex})}(\text{aq}) = -65.4$ kcal/mol, which agrees reasonably with the experimental value of -69.51 kcal/mol.²⁷

Addressing Eq. (4), several approximations have accumulated. The first of those is the neglect of population fluctuation. From Fig. 5, we see that this error amounts to $kT \ln p_{\text{Rb}^+}(\bar{n}) \approx -0.6$ kcal/mol, roughly a 1% error on the predicted hydration free energy. This could be easily appended to the final result, but it is not significant here.

Further approximations entered to evaluate the free energies on the right side of Eq. (4). A normal mode analysis yields harmonic frequencies that are expected to represent the vibrational motions for small ion-water clusters. A perturbative analysis⁷⁶ of anharmonicity in the electronic energy surface confirmed that vibrations in the $\bar{n} = 4$ cluster are well-described by normal mode analysis. If anharmonicity were important, the corrections could easily be included in the final result.

A serious approximation is the treatment of the external environment as a dielectric continuum when considering $\mu_{\text{Rb}(\text{H}_2\text{O})_{\bar{n}}^+}^{(\text{ex})} - n\mu_{\text{H}_2\text{O}}^{(\text{ex})}$. This approximation is clearly not realistic on a molecular scale, *i.e.*, the solvent is *not* actually a dielectric continuum. But in this application, the dielectric continuum model is used for outer-shell electrostatic effects, and thus molecular-scale inaccuracies should be less serious.

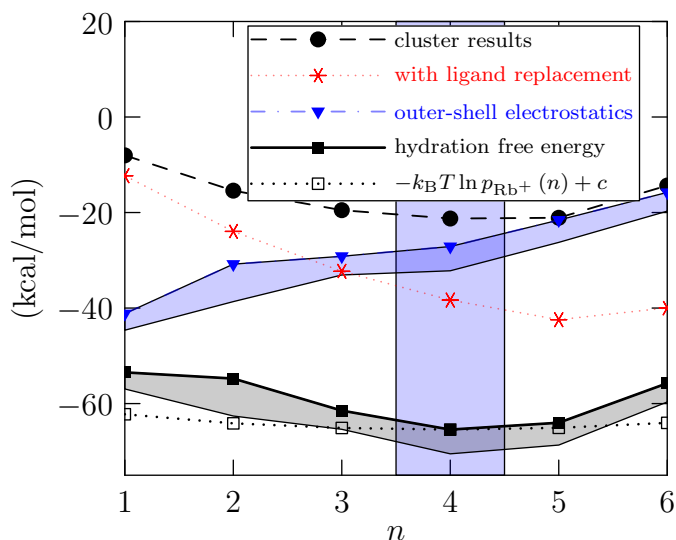


Fig. 6 Contributions from the primitive quasi-chemical evaluation of $\mu_{\text{Rb}^+}^{(\text{ex})}(\text{aq})$. The predicted hydration free energy is -65.4 kcal/mol when the outer-shell electrostatics contribution is based on a *single* $n = \bar{n} = 4$ solvent-adapted cluster configuration. Using instead many configurations sampled from the AIMD simulation record, the outer-shell electrostatics contributions are similar, but slightly lower, and predict $\mu_{\text{Rb}^+}^{(\text{ex})}(\text{aq}) = -70.5$ kcal/mol. The modeled inner-shell occupancy distributions $p_{\text{Rb}^+}(n)$ resemble the observations from the AIMD simulation (Fig. 5, $\lambda = 3.2$ Å), plotted with open boxes where the constant ‘ c ’ is adjusted to match the single-point QCT model at $n = \bar{n} = 4$. This qualitatively satisfactory comparison achieved with both single and multiple solvent-adapted structures (highlighted by shading) stands in contrast with a previous primitive assessment⁷⁰ for $\text{K}^+(\text{aq})$ that is expected to be physically similar. That previous work did not attempt a detailed examination of the theory, nor did it consider specifically a neighborhood analysis (Fig. 2), as has been long customary.^{25,29,56,57,59}

Moreover, because of the balance of free energies in this contribution, there is an opportunity for molecular-scale inaccuracies to cancel to some extent.

It is also remarkable and approximate that we calculated $\mu_{\text{Rb}(\text{H}_2\text{O})_n}^{(\text{ex})}$ on the basis of a *single* cluster configuration and electronic charge distribution. Moreover, we based the estimate of $\mu_{\text{Rb}(\text{H}_2\text{O})_n}^{(\text{ex})}$ on the geometry and electronic charge distribution of the cluster that has been subtly altered by the environment. This inclusion of a solvent reaction field is expected²⁵ to be an improvement for simple dielectric and Gaussian distribution theories of solvation free energies. Further, this approach represents a distinct change from typical procedures used previously.²⁵ Although the cluster structures ($n=1-8$) are only subtly different on the basis of casual inspection, the results of Fig. 6 for $n \geq 5$ are decisively improved. With previous procedures, the present results become qualitatively like the published, and puzzling, results for K^+ with $n \geq 5$.²⁵ Of course, the similarity of Rb^+ and K^+ is the natural physical expectation. The implied computed hydration free energy based on $\bar{n} = 4$ is not much changed in quality compared to estimates based on the earlier procedures,²⁵ as also noted previously.⁵⁷ For example, $\mu_{\text{Rb}^+}^{(\text{ex})}$ is only 2 kcal/mol more positive using Eq. 4 based on a single cluster geometry and electronic charge distribution independent of the environment. The difference here is that now the overall occupancy distribution (Fig. 6) is also qualitatively reasonable.

This *single-point* estimate of the cluster free energy was tested by sampling inner-shell structures from the AIMD simulation record and evaluating electrostatic contributions to the free energies using a simple dielectric continuum solvation model. In that case, the excess free energies of the sampled clusters and individual water ligands were estimated using the APBS-version 1.3 software⁷⁷ with the same parameters described earlier.⁵⁷ Results for the sampled clusters were then combined in the thermodynamically consistent fashion, *i.e.*, by adding the inverses of the Boltzmann factors. That test produced slightly lower outer-shell electrostatic contributions and $\mu_{\text{Rb}^+}^{(\text{ex})}(\text{aq}) = -70.5$ kcal/mol, thus confirming the results above. The conclusion appears to be that isolated $n \geq 5$ clusters are sufficiently unusual in structure to cause trouble for single-point estimates of $\mu_{\text{Rb}(\text{H}_2\text{O})_n}^{(\text{ex})}$ based on gas-phase structures. Single solvent-adapted structures, or structures sampled from liquid-phase simulations, result in a satisfactory improvement.

5 Concluding Discussion

Using AIMD simulation and primitive quasi-chemical theory, we find that $n = 4$ waters preferentially solvate Rb^+ within a spherical inner shell defined by radius $\lambda = 3.2$ Å. This boundary extends slightly beyond the first peak of the Rb-O radial

distribution function observed in AIMD simulations and reported in experiments ($r = 3.0 \text{ \AA}$), but lies well within the putative minimum at $r = 3.8 \text{ \AA}$ occupied by $n = 7$ waters. As customary, we intentionally chose a smaller inner hydration shell for free energy analysis to avoid split occupancy between first and second hydration shells observed for the 7th-most distant water from Rb^+ in AIMD simulations.

The hydration free energy for Rb^+ predicted by primitive quasi-chemical evaluation agrees reasonably well with experiment. Good agreement is achieved when treating the most probable aqueous coordination complex within the defined inner hydration shell as a *single* energy-optimized gas-phase species using quantum mechanical methods and coupling that cluster to an implicit model of the solution. For example, coupling $\text{Rb}^+(\text{H}_2\text{O})_4$ to a dielectric continuum model, whether or not the cluster adapts to that environment, results in a hydration free energy of $\approx -65 \text{ kcal/mol}$. In comparison, coupling many $n = 4$ configurations sampled from AIMD simulation to an implicit solvation model results in a similar hydration free energy prediction of -70.5 kcal/mol , a result within 1 kcal/mol of experiment.

Although the overall hydration free energy remains similar, a significant improvement does occur in the distribution of inner-shell coordinations predicted when treating solvent-adapted clusters (one or many) compared to prior procedures that treated only gas-phase clusters. Comparison of the occupancy distribution from AIMD with those from a LJ model indicates that AIMD results exhibit slightly lower coordination numbers with greater variability.

Based on similarity in size (within 0.2 \AA) and identical charge, Rb^+ and K^+ ions are expected to share similar solvation characteristics in water and other environments. Foremost, hydration free energies are nearly identical according to experiments, a result also predicted by quasi-chemical analyses. Further similarities can be highlighted by comparing AIMD simulation and quasi-chemical free energy analysis of Rb^+ with earlier studies of K^+ .^{25,29,56,57,59} For example, the first peaks in ion-O radial distribution functions fall in similar locations, but slightly closer for the smaller K^+ ion ($r = 2.8 \text{ \AA}$), as anticipated. In both cases, a weak minimum obscures identification of a coordination shell. For K^+ , this minimum ostensibly occurs closer ($r = 3.5 \text{ \AA}$) with occupation by $n = 6$ waters, one less than Rb^+ . Similar to Rb^+ , split occupancy observed in the AIMD record of $\text{K}^+(\text{aq})$ simulations, specifically relating to the 6th-most distant water, motivated definition of a more restricted inner hydration shell for free energy analysis.

Perhaps unexpectedly, these inner shells are defined at nearly identical distances for Rb^+ and K^+ ions ($\lambda_{\text{K}^+} = 3.1 \text{ \AA}$) and have similar properties: the first $n=1-4$ waters fill-in the first peaks in the ion-oxygen radial distribution functions, and $n=4$ waters preferentially solvate both K^+ and Rb^+ according

to AIMD simulation and quasi-chemical analysis. In contrast, $n=4$ waters fill-in the first peak and preferentially solvate Na^+ within a closer inner-shell distance of $\lambda = 2.6 \text{ \AA}$.^{25,57} Finally, stable inner-shell hydration structures for both K^+ and Rb^+ exist in gas phase that are absent in AIMD simulations of the liquid phase. For example, the $n = 8$ non-split occupancy is a rare composition in AIMD simulation, but forms a stable skewed cubic structure with 4 waters in a plane above and 4 below K^+ ⁵⁷ and Rb^+ ⁷⁸ in the absence of stabilizing interactions with the more distant solvation environment. This high coordination contrasts with smaller inner-shell coordinations ($n \leq 6$) reported for Na^+ .^{25,57} Further, these 8-coordinate clusters resemble the crystallographic ligands resolved around K^+ and Rb^+ ions in the binding sites of potassium ion channels that conduct K^+ and Rb^+ , but reject smaller Na^+ ions.^{10,79} Following previous studies of selective K^+ and Na^+ binding,^{9,57,59,60} quasi-chemical theory may be useful in future work to analyze the subtleties of Rb^+ binding and conduction in potassium channels.

Quasi-chemical theory applied to ion hydration combines statistical mechanical theory, electronic structure calculations, and molecular simulation, disciplines which are individually subjects for specialized professional attention. Because it combines activities which are themselves non-trivial, quasi-chemical theory is typically viewed with surprise. Nevertheless, it provides a fully-considered framework for analysis of ion hydration.

It is striking that the three sub-disciplines noted (statistical mechanical theory, electronic structure calculations, and molecular simulation) are so distinct. Typical practice in each subdiscipline is to parameterize the ingredients from the other two in order to eliminate those complexities. Thus, for example, sophisticated electronic structure calculations are done with solution models (dielectric continuum models) that are not justified on the basis of more basic observation. Similarly, sophisticated statistical mechanical theory is typically pursued where molecular-scale realism of the model can be empirically eliminated, for example by treating parameterized pair-decomposable models of intermolecular interactions. Simulation calculations also, of course, adopt extensively parameterized models. But they also have the limitation of being non-theoretical, *i.e.*, not requiring physical insight they most often do not result in any. Indeed, simulations can be high-resolution experiments of undetermined accuracy for any physical system.

Quasi-chemical theory is not a *take-it-or-leave-it* model, and not a series expansion, but a well-defined structure for combining computational results from distinct sources that treat separately near and more distant neighbors. As more advanced applications are encountered — here with the $\text{Rb}^+(\text{aq})$, which localizes near-neighbor water molecules slightly less definitely than some less advanced cases — some physical

learning and judgement is required. A big step in that learning has been to categorize near-neighbors on the basis of the neighborhood decomposition of the radial distribution as in Fig. 2. This is in contrast to identification of neighbors on the basis of the location of the first minimum of that radial distribution, which is often less than compelling. Another step in that learning has been to consider more sophisticated procedures for estimation of cluster hydration free energies. Our discussion here has emphasized further the clear learning point that fluctuations of the *composition* of the inner-shell are numerically non-significant for strongly bound cases such as Rb^+ and where a well-informed identification of inner-shell ligands has been achieved.

Acknowledgment

Sandia National Laboratories is a multiprogram laboratory managed and operated by Sandia Corporation, a wholly owned subsidiary of Lockheed Martin Corporation, for the U.S. Department of Energy's National Nuclear Security Administration under Contract DE-AC04-94AL8500. This work was supported by Sandia's LDRD program and by the National Science Foundation under the NSF EPSCoR Cooperative Agreement No. EPS-1003897, with additional support from the Louisiana Board of Regents.

References

- 1 J. J. O'Shea and R. G. Jones, *Nature*, 2013.
- 2 M. Kleinewietfeld, A. Manzel, J. Titze, H. Kvakan, N. Yosef, R. A. Linker, D. N. Muller and D. A. Hafler, *Nature*, 2013.
- 3 C. Wu, N. Yosef, T. Thalhamer, C. Zhu, S. Xiao, Y. Kishi, A. Regev and V. K. Kuchroo, *Nature*, 2013.
- 4 N. Yosef, A. K. Shalek, J. T. Gaubblomme, H. Jin, Y. Lee, A. Awasthi, C. Wu, K. Karwacz, S. Xiao, M. Jorgolli, D. Gennert, R. Satija, A. Shakya, D. Y. Lu, J. J. Trombetta, M. R. Pillai, P. J. Ratcliffe, M. L. Coleman, M. Bix, D. Tantin, H. Park, V. K. Kuchroo and A. Regev, *Nature*, 2013.
- 5 M. D. Cahalan and K. G. Chandy, *Immunol. Rev.*, 2009, **231**, 59–87.
- 6 C. Beeton, H. Wulff, N. E. Standifer, P. Azam, K. M. Mullen, M. W. Pennington, A. Koksiki-Andreaco, E. Wei, A. Grino, D. R. Counts, P. H. Wang, C. J. LeeHealey, B. S. Andrews, A. Sankaranarayanan, D. Homerick, W. W. Roeck, J. Tehranzadeh, K. L. Stanhope, P. Zimin, P. J. Havel, S. Griffey, H.-G. Knaus, G. T. Nepom, G. A. Gutman, P. A. Calabresi and K. G. Chandy, *Proc. Natl. Acad. Sci. USA*, 2006, **103**, 17414–9.
- 7 B. Hille, *Ionic Channels of Excitable Membranes*, Sinauer Associates, Sunderland, MA, 3rd edn, 2001.
- 8 O. Andersen, *J. Gen. Physiol.*, 2011, **137**, 393.
- 9 S. Varma, D. M. Rogers, L. R. Pratt and S. B. Rempe, *J. Gen. Physiol.*, 2011, **137**, 479–488.
- 10 J. H. Morales-Cabral, Y. Zhou and R. MacKinnon, *Nature*, 2001, **414**, 37–42.
- 11 X. Tao, J. L. Avalos, J. Chen and R. MacKinnon, *Science*, 2009, **326**, 1668–1674.
- 12 T. L. Beck, M. E. Paulaitis and L. R. Pratt, *The Potential Distribution Theorem and Models of Molecular Solutions*, Cambridge University Press, 2006.
- 13 J. Shah, D. Asthagiri, L. R. Pratt and M. Paulaitis, *J. Chem. Phys.*, 2007, **127**, 144508.

-
- 14 S. Chempath, L. R. Pratt and M. E. Paulaitis, *Chem. Phys. Letts.*, 2010, **487**, 24–27.
- 15 F. H. Stillinger, *Science*, 1980, **209**, 451–457.
- 16 B. Widom, *Science*, 1967, **157**, 375–382.
- 17 D. Chandler, J. D. Weeks and H. C. Andersen, *Science*, 1983, **220**, 787–794.
- 18 D. T. Bowron, A. Filipponi, M. A. Roberts and J. L. Finney, *Phys. Rev. Letts.*, 1998, **81**, 4164–4167.
- 19 H. S. Ashbaugh, D. Asthagiri, L. R. Pratt and S. B. Rempe, *Biophys. Chem.*, 2003, **105**, 323–338.
- 20 R. L. Martin, P. J. Hay and L. R. Pratt, *J. Phys. Chem. A*, 1998, **102**, 3565.
- 21 L. R. Pratt and R. A. LaViolette, *Mol. Phys.*, 1998, **94**, 909–915.
- 22 L. R. Pratt and S. B. Rempe, *Simulation and Theory of Electrostatic Interactions in Solution*, AIP Conf. Proc., New York, 1999, vol. 492, p. 172.
- 23 M. E. Paulaitis and L. R. Pratt, *Adv. Protein Chem.*, 2002, **62**, 283.
- 24 L. R. Pratt and D. Asthagiri, *Free Energy Calculations. Theory and Applications in Chemistry and Biology*, Springer, Berlin, 2006, ch. 9. Potential distribution methods and free energy models of molecular solutions.
- 25 D. M. Rogers, D. Jiao, L. R. Pratt and S. B. Rempe, *Annual Reports in Computational Chemistry*, Elsevier, New York, 2012, vol. 8, ch. 4, pp. 71–127.
- 26 S. B. Rempe, L. R. Pratt, G. Hummer, J. D. Kress, R. L. Martin and A. Redondo, *J. Am. Chem. Soc.*, 2000, **122**, 966.
- 27 Y. Marcus, *J. Chem. Soc. Faraday Trans.*, 1991, **87**, 2995.
- 28 K. Leung, S. B. Rempe and A. von Lilienfeld, *J. Chem. Phys.*, 2009, **130**, 204507–204518.
- 29 S. Varma and S. B. Rempe, *Biophys. Chem.*, 2006, **124**, 192.
- 30 P. E. Mason, S. Ansell and G. W. Neilson, *J. Phys.: Condens. Matter*, 2006, **18**, 8437–8447.
- 31 D. Asthagiri, P. D. Dixit, S. Merchant, M. E. Paulaitis, L. R. Pratt, S. B. Rempe and S. Varma, *Chem. Phys. Letts.*, 2010, **485**, 1–7.
- 32 G. Kresse and J. Hafner, *Phys. Rev. B*, 1993, **47**, RC558.
- 33 G. Kresse and J. Furthmüller, *Phys. Rev. B*, 1996, **54**, 11169.
- 34 Y. Wang and J. P. Perdew, *Phys. Rev. B*, 1991, **44**, 13298.
- 35 J. P. Perdew, J. A. Chevary, S. H. Vosko, K. A. Jackson, M. R. Pederson, D. J. Singh and C. Fiolhais, *Phys. Rev. B*, 1992, **46**, 6671.
- 36 P. E. Blöchl, *Phys. Rev. B*, 1994, **50**, 17953.
- 37 A. Bankura, V. Carnevale and M. L. Klein, *J. Chem. Phys.*, 2013, **138**, 014501.
- 38 E. Schwegler, J. C. Grossman, F. Gygi and G. Galli, *J. Chem. Phys.*, 2004, **121**, 5400–5409.
- 39 J. VandeVondele, F. Mohamed, M. Krack, J. Hutter, M. Sprik and M. Parrinello, *J. Chem. Phys.*, 2005, **122**, 14515.
- 40 K. Leung and S. B. Rempe, *Phys. Chem. Chem. Phys.*, 2006, **8**, 2153–2162.
- 41 S. B. Rempe, T. R. Mattsson and K. Leung, *Phys. Chem. Chem. Phys.*, 2008, **10**, 4685–4687.
- 42 J. Åqvist, *J. Phys. Chem.*, 1990, **94**, 8021.
- 43 H. J. C. Berendsen, J. R. Grigera and T. P. Straatsma, *J. Phys. Chem.*, 1987, **91**, 6269.
- 44 E. Lindahl, B. Hess and D. van der Spoel, *Journal Mol. Mod.*, 2001, **7**, 306.
- 45 S. Miyamoto and P. A. Kollman, *J. Comput. Chem.*, 1992, **13**, 952.
- 46 S. Nose, *Mol. Phys.*, 1984, **52**, 255.
- 47 S. Nose, *J. Chem. Phys.*, 1984, **81**, 511.
- 48 W. G. Hoover, *Phys. Rev. A*, 1985, **31**, 1695.
- 49 D. Asthagiri, L. R. Pratt, M. Paulaitis and S. B. Rempe, *J. Am. Chem. Soc.*, 2004, **126**, 1285–1289.
- 50 D. Jiao, K. Leung, S. B. Rempe and T. M. Nenoff, *J. Chem. Theo. Comp.*, 2011, **7**, 485–495.
- 51 S. Varma and S. B. Rempe, *Biophys. J.*, 2010, **99**, 3394–3401.
- 52 D. Jiao and S. B. Rempe, *J. Chem. Phys.*, 2011, **134**, 224506.
- 53 D. M. Rogers and S. B. Rempe, *J. Phys. Chem. B*, 2011, **115**, 9116–9129.
- 54 S. B. Rempe and L. R. Pratt, *Fluid Phase Equilib.*, 2001, **183-184**, 121.
- 55 D. Asthagiri, L. R. Pratt and H. Ashbaugh, *J. Chem. Phys.*, 2003, **119**, 2702–8.
- 56 S. B. Rempe, D. Asthagiri and L. R. Pratt, *Phys. Chem. Chem. Phys.*, 2004, **6**, 1966.
- 57 S. Varma and S. B. Rempe, *J. Am. Chem. Soc.*, 2008, **130**, 15405–15419.
- 58 D. Asthagiri, L. R. Pratt, J. D. Kress and M. A. Gomez, *Proc. Natl. Acad. Sci. USA*, 2004, **101**, 7229–7233.
- 59 S. Varma and S. B. Rempe, *Biophys. J.*, 2007, **93**, 1093–1099.
- 60 S. Varma, D. Sabo and S. B. Rempe, *J. Mol. Biol.*, 2008, **376**, 13.
- 61 D. Sabo, S. Varma, M. G. Martin and S. B. Rempe, *J. Phys. Chem. B*, 2008, **112**, 867–876.
- 62 D. Jiao and S. B. Rempe, *Biochemistry*, 2012, **51**, 5979–5989.
- 63 S. Mazur, *J. Chem. Phys.*, 1992, **97**, 9276.
- 64 M. J. Frisch, G. W. Trucks, H. B. Schlegel, G. E. Scuseria, M. A. Robb, J. R. Cheeseman, J. A. Montgomery, Jr., T. Vreven, K. N. Kudin, J. C. Burant, J. M. Millam, S. S.

-
- Iyengar, J. Tomasi, V. Barone, B. Mennucci, M. Cossi, G. Scalmani, N. Rega, G. A. Petersson, H. Nakatsuji, M. Hada, M. Ehara, K. Toyota, R. Fukuda, J. Hasegawa, M. Ishida, T. Nakajima, Y. Honda, O. Kitao, H. Nakai, M. Klene, X. Li, J. E. Knox, H. P. Hratchian, J. B. Cross, V. Bakken, C. Adamo, J. Jaramillo, R. Gomperts, R. E. Stratmann, O. Yazyev, A. J. Austin, R. Cammi, C. Pomelli, J. W. Ochterski, P. Y. Ayala, K. Morokuma, G. A. Voth, P. Salvador, J. J. Dannenberg, V. G. Zakrzewski, S. Dapprich, A. D. Daniels, M. C. Strain, O. Farkas, D. K. Malick, A. D. Rabuck, K. Raghavachari, J. B. Foresman, J. V. Ortiz, Q. Cui, A. G. Baboul, S. Clifford, J. Cioslowski, B. B. Stefanov, G. Liu, A. Liashenko, P. Piskorz, I. Komaromi, R. L. Martin, D. J. Fox, T. Keith, M. A. Al-Laham, C. Y. Peng, A. Nanayakkara, M. Challacombe, P. M. W. Gill, B. Johnson, W. Chen, M. W. Wong, C. Gonzalez and J. A. Pople, *Gaussian 09, Revision C.01*, Gaussian, Inc., Wallingford, CT, 2009.
- 65 A. D. Becke, *J. Chem. Phys.*, 1993, **98**, 5648.
- 66 C. Lee, W. Yang and R. G. Parr, *Phys. Rev. B*, 1988, **37**, 785.
- 67 E. B. Wilson, J. C. Decius and P. Cross, *Molecular Vibrations*, McGraw-Hill, New York, 1955.
- 68 S. Rempe and H. Jónsson, *Chem. Ed.*, 1998, **3**, 04231–6.
- 69 D. A. McQuarrie, *Statistical Mechanics*, Harper & Row, New York, 1976.
- 70 B. Roux and H. Yu, *J. Chem. Phys.*, 2010, **132**, 234101.
- 71 J. Tomasi, B. Mennucci and R. Cammi, *Chem. Rev.*, 2005, **105**, 2999–3093.
- 72 G. Scalmani and M. J. Frisch, *J. Chem. Phys.*, 2010, **132**, 114110 (1–15).
- 73 J. L. Fulton, D. M. Pfund, S. L. Wallen, M. Newville, E. A. Stern and Y. Ma, *J. Chem. Phys.*, 1996, **105**, 2161.
- 74 A. Filipponi, S. D. Panfilis, C. Oliva, M. A. Ricci, P. D'Angelo and D. T. Bowron, *Phys. Rev. Lett.*, 2003, **91**, 165505.
- 75 S. Ramos, A. C. Barnes, G. W. Neilson and M. J. Capitan, *Chem. Phys.*, 2000, **258**, 171.
- 76 V. Barone, *J. Chem. Phys.*, 2005, **122**, 014108.
- 77 N. A. Baker, D. Sept, S. Joseph, M. J. Holst and J. A. McCammon, *Proc. Natl. Acad. Sci. U.S.A.*, 2001, **98**, 10037.
- 78 M. L. San-Román, J. Hernández-Cobos, H. Saint-Martin and I. Ortega-Blake, *Theoretical Chemistry Accounts*, 2009, **126**, 197–211.
- 79 Y. Zhou, J. Morals-Cabral, A. Kaufman and R. MacKinnon, *Nature*, 2001, **414**, 43–48.